Identification and characterization of developmental genes in streptomyces

Zhang, L.

V

The Lcm proteins control spore wall integrity of *Streptomyces*

Le Zhang, Joost Willemse, Changsheng Wu, Young H. Choi and Gilles P. van Wezel

ABSTRACT

Streptomycetes are mycelial microorganisms that reproduce by sporulation. Studying spontaneous mutants with defects in morphogenesis is a promising approach to find novel genes that control growth and/or development. Here we show that the spontaneous mutant *Streptomyces griseus* SY1, which hyper-sporulates in submerged cultures, has a nonsense mutation in the first gene of the *lcmABC* operon, which is widely distributed among the actinobacteria and was previously implicated in cell division in *Bacillus*. Deletion of the *lcmABC* gene cluster or recreating the nonsense mutation in *lcmA* in *S. griseus* or our model strain *Streptomyces coelicolor* resulted in accelerated growth and development on solid media, with longer spores with a thinner spore wall, which were sensitive to heat. Defective septum synthesis was frequently observed in the mutants. LcmA, LcmB and LcmC localized as a regular pattern of foci in young aerial hyphae, and then localized at the septum during sporulation-specific cell division, whereby LcmB overlapped the entire septum, while LcmA and LcmC crossed the septum at a 45º angle, perhaps forming a complex at the site of septum closure. NMR-based metabolomic analysis showed significant changes in terms of primary metabolite composition in *lcmABC* and *lcmA** mutants. Our data show that LcmA, LcmB and LcmC are novel cell division-related proteins in *Streptomyces* that are required for spore integrity.

INTRODUCTION

Actinomycetes are important industrial microorganisms as producers of a wide variety of natural products, including antibiotics, anticancer agents and immunosuppressants (Hopwood, 2007), as well as many industrially relevant enzymes (Vrancken and Anné, 2009). Of the actinomycetes, the streptomycetes produce around half of all known antibiotics. Streptomycetes are mycelial microorganisms not dissimilar to filamentous fungi in their morphology, and undergo a complex multicellular life cycle (Claessen *et al.*, 2014). After germination of a spore, a branched vegetative mycelium is formed that consists of multinucleoid compartments separated by cross-walls (Chater and Losick, 1997). In the reproductive phase, triggered by adverse conditions such as nutrient depletion, aerial hyphae are formed that eventually differentiate into long chains of spores.

In submerged cultures streptomycetes grow as mycelial networks, and often form large mycelial pellets. However, a number of streptomycetes, including the streptomycin producer *Streptomyces griseus* and the chloramphenicol producer *Streptomyces venezuelae*, show more dispersed growth and can sporulate in submerged culture (Girard *et al.*, 2013). The process of submerged sporulation has not been studied extensively, but is important for our understanding of sporulation-specific cell division; it allows the identification of genes that affect sporulation-specific cell division but not aerial hyphae formation (Reviewed in (van Dissel *et al.*, 2014)). Besides the important fundamental implications, knowledge of the genes that control liquid-culture morphogenesis can also be exploited for directed strain evolution at the molecular level for industrial application.

To obtain more information on genes that play a role in submerged sporulation and cell division of streptomycetes, studying spontaneous mutants is an attractive approach, in particular now genome sequencing and comparison has become feasible. One such mutant is strain SY1 of *Streptomyces griseus*, which was derived as a fragmenting variant of *S. griseus* NRRL B2682 by random mutagenesis (Kawamoto and Ensign, 1995). While the parental strain only sporulates after nutritional shift-down from rich to poor media, its derivative SY1 also sporulates in rich cultures, similarly to *S. venezuelae*. On studying *S. griseus* SY1 in more detail, we previously reported that the strain produces enhanced levels of the cell division activator protein SsgA, which is important for sporulation in surface- and liquid-grown cultures (van Wezel *et al.*, 2000b). Members of the family of SsgA-like proteins exclusively occur in actinomycetes, and the number of paralogs in an organism directly relates to

the morphogenesis (Jakimowicz and van Wezel, 2012; Traag and van Wezel, 2008). Overexpression of SsgA from *S. griseus* in *S. coelicolor* induces mycelial fragmentation and spore formation in submerged cultures (van Wezel *et al.*, 2000b). This was applied in industrial fermentations to obtain improved growth and enzyme production during fermentation (van Wezel *et al.*, 2006). Of the SALPs, *ssgA, ssgB* and *ssgG* control septum-site localization in streptomycetes, whereby *ssgA* and *ssgB* are essential for sporulation (Keijser *et al.*, 2003; Sevcikova and Kormanec, 2003; van Wezel *et al.*, 2000b).

Understanding the nature of the mutation in *S. griseus* SY1, could better our understanding of the control of submerged sporulation and cell division in streptomycetes. In this work compared the genomes of *S. griseus* SY1 with its parent B2682, which identified several SNPs, including a mutation in a putative sporulation-related gene SCO1387 that resulted in a premature stop codon after the sixth codon position. SCO1387 is the first gene of a likely operon of three genes encoding membrane proteins of unknown function, which we renamed *lcmABC* (for liquid culture morphology). LcmB was previously implicated as a sporulation-related protein in *Bacillus subtilis* (Beall and Lutkenhaus, 1989). In this work, we show that the Lcm proteins play a role in morphogenesis probably via affecting spores composition.

MATERIALS AND METHODS

Bacterial strains and media

Bacterial strains used in this work are listed in Table 1. *Escherichia coli* strains JM109 (Sambrook *et al.*, 1989) was used for routine cloning procedures, *E. coli* ET12567 (MacNeil *et al.*, 1992; Kieser *et al.*, 2000) was used for obtaining non-methylated DNA isolation for efficient *S. coelicolor* transformation and *E. coli* IR539 (Suzuki *et al.*, 2011) for preparing DNA for efficient transformation of *S. griseus*. *E.coli* transformants were selected on LB agar containing the appropriate antibiotics and grown O/N at 37°C (Sambrook *et al.*, 1989). *Streptomyces coelicolor* A3(2) M145 and *Streptomyces griseus* IFO13350 were the parents for the mutants. YMPD (Ohnishi *et al.*, 1999) or TSBS (tryptone soy broth (Difco) containing 10% (w/v) sucrose) were used for standard cultivation as described (Kieser *et al.*, 2000). R5 agar plates were used for regeneration of protoplasts and - after addition of antibiotics - to select recombinants, and SFM (soy flour mannitol) and MM (minimal media) agar plates for preparing spores suspensions, and for morphological characterization and microscopy of all strains (Kieser *et al.*, 2000).

Plasmids and constructs

Plasmids and constructs used in this work are summarized in Table 2, all oligonucleotides are listed in Table 3.

Constructs for creating mutants and for complementation

The strategy for creating knock-out mutants was described previously (Świątek *et al.*, 2012). The method is based on the multi-copy shuttle vector pWHM3 (Vara *et al.*, 1989), which is an unstable multi-copy vector that is easily lost when selection is relieved (van Wezel *et al.*, 2005). For the deletion of *lcmA*, plasmid pGWS736 was created. For this, the -1496/+6 upstream region (nt numbering relative to the start of *lcmA*) was amplified by PCR from *S. coelicolor* M145 genomic DNA using primer pairs lcmA_LF-1496 and lcmA_LR+6, and the downstream region +832/+2232 was amplified using primer pair lcmA_RF+832 and lcmA_RR+2232. The PCR-amplified upstream and downstream regions were digested with EcoRI and XbaI, and with XbaI and HindIII, respectively, and ligated in a three-fragment ligation into EcoRI/HindIII-digested vector pWHM3. The unique XbaI site engineered in-between the flanking regions allows insertion of the apramycin resistance cassette *aac(3)IV* flanked by *loxP* recognition sites. The presence of *loxP* sites allows

efficient removal of the apramycin resistance cassette by expression of the Cre-recombinase by introducing plasmid pUWL-Cre, which then generates a marker-less deletion mutant (Fedoryshyn *et al.*, 2008). Essentially the same strategy was used to create gene deletion constructs pGW738, pGWS739, and pGWS740 for the gene replacement of *lcmB*, *lcmC*, and the whole *lcmABC* gene cluster, respectively. pGWS738 contains the -1483/+60 and +274/+1832 regions relative to the start of *lcmB*, pGWS739 contains the -1396/+45 and +847/+2177 regions relative to the start of *lcmC*, and pGWS740 contains the -1496/+6 region relative to *lcmA* and the downstream +847/+2177 region relative to *lcmC*. All constructs contained the apramycin resistance cassette flanked by *loxP* sites for selection of mutants and subsequent removal to create markerless deletion mutants.

Construct pWGS737 was designed to replace the 7th codon position of *lcmA* by a stop codon, corresponding to the spontaneous mutation found in *S. griseus* SY1. pGWS737 contains -1496/+21 and +22/+2232 regions relative to *lcmA,* with the apramycin resistance cassette flanked by *loxP* sites inserted in-between. Regions -1496/+21 and +22/+2232 relative to *lcmA* were amplified using primer pairs lcmA_LF-1496 and lcmA_LR+21 and lcmA_RF+22 and lcmA_RR+2232, respectively. Primers lcmA_LR+21 contains mutation at amino acid position 7 of *lcmA*; CCA was changed to TGA (proline was changed to stop codon). Using a similar approach, plasmids pGWS741, pGWS742 and pGWS743 were created, for the deletion of *lcmA*, to create a non-sense mutation at the 7th codon position in *lcmA* and to delete *lcmABC*, respectively, in strain *S. griseus* IFO13350.

For complementation of the mutants of *S.coelicolor* M145 construct pGWS778 was made which is based on the integrative vector pSET152 (Bierman *et al.*, 1992). For this, the entire *lcmABC* gene cluster (including promoter region) was amplified by PCR using primer pair lcmB_LF-1483 and lcmB_R+1326, and inserted into EcoRI/XbaI-digested pSET152. The construct harbors the entire *lcmABC* gene cluster including 580 bp of upstream and 140 nt downstream region and expresses *lcmABC* from the natural promoter.

Constructs for translational fusion of LcmABC with eGFP

To obtain a construct expressing LcmA-eGFP, we used plasmid pKF41 which expresses FtsZ-eGFP from the native *ftsZ* promoter region (Grantcharova *et al.*, 2005). The insert was excised with BglII and NotI, cloned into the integrative vector pSET152 and the coding region of *ftsZ* was replaced by that of *lcmA*. For this, the vector was digested with StuI and BamHI, the *lcmA*

gene was PCR-amplified from the genome of *S. coelicolor* using primer pair lcmA_F+1 and lcmA_R+903, and cloned as a StuI-BglII fragment in-between *ftsZ*p and *egfp* to generate pGWS768. Using the same strategy, pGWS769 and pGWS770 were constructed for in frame fusion of *lcmB-egfp* and *lcmC-egfp* using primer pairs lcmB_F+1 and lcmB_R+330 and lcmC_F+1 and lcmC_R+852, respectively.

Table 1. Bacterial strains

Bacteria strains	Genotype	Reference
E. coli JM109	See reference	(Sambrook *et al.*, 1989)
E. coli ET12567	See reference	(MacNeil *et al.*, 1992)
E. coli IR539	See reference	(Suzuki *et al.*, 2011)
S. coelicolor M145	$SCP1^{-}$ $SCP2^{-}$	(Kieser *et al.*, 2000)
S. griseus IFO13350	See reference	(Ohnishi *et al.*, 2008)
GAL56	M145 Δ*lcmA*	This work
GAL57	M145 Δ*lcmB*	This work
GAL58	M145 Δ*lcmC*	This work
GAL59	M145 *lcmA** (7^{th} AA changed to stop codon)	This work
GAL60	M145 Δ*lcmABC*	This work
GAL61	M145 Δ*gcvP* (::*aac(3)IV*)	This work
GAL56-sg	IFO13350 Δ*lcmA*	This work
GAL59-sg	IFO13350 Δ*lcmA**	This work
GAL60-sg	IFO13350 Δ*lcmABC*	This work
GAL64	M145 + pGWS768	This work
GAL65	M145 + pGWS769	This work
GAL66	M145 + pGWS770	This work
GAL68	GAL59 + pGWS778	This work
GAL69	GAL60 + pGWS778	This work
ΔUTR-T	*S. griseus* IFO13350 with deletion of 5'-untranslated region of *gcvTH*	(Tezuka and Ohnishi, 2014)
ΔUTR-P	*S. griseus* IFO13350 with deletion of 5'-untranslated region of *gcvP*	(Tezuka and Ohnishi, 2014)
ΔUTR-PΔUTR-T	*S. griseus* IFO13350 with deletion of 5'-untranslated regions of *gcvP* and *gcvTH*	(Tezuka and Ohnishi, 2014)

Table 2. Plasmids and Constructs

Plasmid and constructs	Description	Reference
pWHM3	*E. coli*/*Streptomyces* shuttle vector, high copy number but unstable in *Streptomyces*	(Vara *et al.*, 1989)
pSET152	*E. coli*/*Streptomyces* shuttle vector, high copy number in E. coli and integrative in Streptomyces	(Bierman *et al.*, 1992)
pUWL-Cre	plasmid expressing Cre-recombinase	(Fedoryshyn *et al.*, 2008)
pGWS736	pWHM3 containing flanking regions of *S. coelicolor* SCO1387 with apra*loxP* inserted in-between	This work
pGWS737	pWHM3 containing regions -1496/+21 and +22/+2232 relative to SCO1387 with apraloxP-XbaI inserted between and with non-sense mutation at 7th amino acid position of SCO1387	This work
pGWS738	pWHM3 containing flanking regions of *S. coelicolor* SCO1386 with apra*loxP* inserted in-between	This work
pGWS739	pWHM3 containing flanking regions of *S. coelicolor* SCO1385 with apra*loxP* inserted in-between	This work
pGWS740	pWHM3 containing upstream region of *S. coelicolor* SCO1387 and downstream region of *S. coelicolor* SCO1385 with apra*loxP* inserted in-between in pWHM3	This work
pGWS752	pWHM3 containing flanking regions of *S. coelicolor* SCO1378 with apra*loxP* inserted in-between	This work
pGWS741	pWHM3 containing flanking regions of *S. griseus* SGR_6142 with apra*loxP* inserted in-between	This work
pGWS742	pWHM3 containing Regions -1473/+21 and +22/+2312 relative to SGR_6142 apra*loxP* inserted in-between and with non-sense mutation at 7th amino acid position of SGR_6142	This work
pGWS743	pWHM3 containing upstream region of *S. griseus* SGR_6142 and downstream region of *S. griseus* SGR_6144 with apra*loxP* inserted in-between	This work
pGWS768	pSET152 harboring *lcmA* and *egfp* under control of the *ftsZ* promoter	This work
pGWS769	pSET152 harboring *lcmB* and *egfp* under control of the *ftsZ* promoter	This work
pGWS770	pSET152 harboring *lcmC* and *egfp* under control of the *ftsZ* promoter	This work
pGWS778	pSET152 with 2.8kb fragment harboring *lcmABC* cluster and its native promoter region	This work

Table 3. Oligonucleotides

Name	5'-3' sequence[#]
lcmA_LF-1496	GTCA**GAATTC**GCGCGTTCGTCAACACCTCGGTG
lcmA_LR+6	GTCAGAAGTTATCCATCACC**TCTAGA**GCACATCGTCGCACGCCACCGCCA
lcmA_RF+832	GTCAGAAGTTATCGCGCATC**TCTAGA**GACCTCAAGCTGCCGGCCGCACCG
lcmA_RR+2232	GTCA**AAGCTT**AACGCACTGGCCGACCCGGACAC
lcmA_LR+21	GTCAGAAGTTATCCATCACC**TCTAGA**TCACTGCGGCATGCCGCACATCGT
lcmA_RF+22	GTCAGAAGTTATCGCGCATC**TCTAGA**CCCCCCGTTCGGAGCACACCCGGG
lcmB_LF-1483	GTCA**GAATTC**GTACCACGGCACGCAGGTCGAG
lcmB_LR+60	GTCAGAAGTTATCCATCACC**TCTAGA**CTCGGGCCGGACCAGCAATCCGGC
lcmB_RF+274	GTCAGAAGTTATCGCGCATC**TCTAGA**CTCGGCATCCGTATCTTCTCCAAC
lcmB_RR+1832	GTCA**AAGCTT**ATCGCCGTCTGGCCGGTGACCTC
lcmC_LF-1396	GTCA**GAATTC**TCCGCACAGGCGCTGCTGGA
lcmC_LR+45	GTCAGAAGTTATCCATCACC**TCTAGA**CAGCTCCTTGCGCAGCCTGTTCGC
lcmC_RF+847	GTCAGAAGTTATCGCGCATC**TCTAGA**TCCCAGTGAACCGGCGGTGCATGG
lcmC_RR+2177	GTCA**AAGCTT**ACGGCGTCCAGATGCTCACG
lcmB_R+1326	GTCA**TCTAGA**ACGCACTGGCCGACCCGGACAC
gcvP_LF-1309	GTCA**GAATTC**ACTGTCCGGGCGGACCATCG
gcvP_LR+9	GTCAGAAGTTATCCATCACC**TCTAGA**GGCGGTCATTGCGGAGGCCTC
gcvP_RF+2881	GTCAGAAGTTATCGCGCATC**TCTAGA**GACTGAGTCCCGCCAAGAAGG
gcvP_RR+4232	GTCA**AAGCTT**CGACGCCCGTCAGTGGATGC
lcmA-sg_LF-1473	GTCA**GGATCC**ACGTCGAGATCACCCCCGAACTG
lcmA-sg_LR+6	GTCAGAAGTTATCCATCACC**TCTAGA**GCACATCGTCGCACGTCATCACGG
lcmA-sg_RF+850	GTCAGAAGTTATCGCGCATC**TCTAGA**GCCTGATCGTCCGTACAGCAGAG
lcmA-sg_RR+2312	GTCA**AAGCTT**ACTGTTGCTGTCCTCGCGTGCAC
lcmA-sg_LR+21	GTCAGAAGTTATCCATCACC**TCTAGA**CTACTGCGACATGCCGCACATCGT
lcmA-sg_RF+22	GTCAGAAGTTATCGCGCATC**TCTAGA**TCCCCCGATCGGAGCACCGCCCCG
lcmC-sg_RF+811	GTCAGAAGTTATCGCGCATC**TCTAGA**TCCCCGTGAGCCGGCCGAGCGTGA
lcmC-sg _RR+2100	GTCA**AAGCTT**CCCTGATGACCTTCAGCGGCAG
lcmA_F+1	GTCAGAATTC**AGGCCT**TCGACATGTGCGGCATGCCGCAGCCA
lcmA_R+903	GCTAAAGCTT**AGATCT**GATGTGCCCTTCTCGGTTAT
lcmB_ F+1	GTCAGAATTC**AGGCCT**TCGACGTGATCGCCGTACTGGGCCTC
lcmB_R+330	GCTAAAGCTT**GGATCC**GCCCGGAAGACGTGGCGTCG
lcmC_F+1	GTCAGAATTC**AGGCCT**TCGACATGAGCGACGACGAGCAGCCG
lcmC_R+852	GCTAAAGCTT**GGATCC**TGGGAGGACGACCGAGCGTA

[#] Restriction sites are underlined and in bold face. GGATCC, BamHI; AGATCT, BglII; GAATTC, EcoRI; AAGCTT, HindIII; AGGCTT, StuI; TCTAGA, XbaI.

Microscopy

S. coelicolor M145 and its mutant derivatives were grown on SFM agar plates and incubated at 30°C for 5-6 days. Aerial hyphae/ spores of *S. coelicolor* and derivatives were studied by cryo-scanning electron microscopy (SEM) using a JEOL JSM6700F cryo-scanning electron microscope as described (Colson *et al.*, 2008). Thin sections of hyphae and spores were imaged at high resolution by Transmission electron microscopy (TEM) using a FEI Tecnai 12 BioTwin transmission electron microscope (Noens *et al.*, 2005).

Sterile cover slips were inserted into SFM agar plates under a 45 degree angle and *S. coelicolor* strains grown at the intersection angle for 3-5 days at 30°C. Then the cover slips were placed on a microscope slide with 5 µl of PBS for fluorescence and corresponding light micrographs, which were taken with an Axiocam Mrc5 camera at a resolution of 37.5 nm/pixel. FITC-WGA, FM5-95 and DAPI were used for staining of cell wall (peptidoglycan), membrane and DNA respectively. The green fluorescence was imaged using 470/40 nm band pass (bp) excitation and 525/50 bp detection; the red images were created using 550/25 nm bp excitation and 625/70 nm bp detection; DNA staining with DAPI was visualized using 370/40 nm excitation with 445/50 nm emission band filter (Willemse and van Wezel, 2009). Images were processed using Adobe Photoshop CS4.

Computer analysis

DNA and protein database searches were done using StrepDB (http://strepdb.streptomyces.org.uk). Phylogenetic relationship analyses and homology searched were performed using STRING (http://string.embl.de). Putative transmembrane domains were identified using transmembrane prediction server DAS (http://www.sbc.su.se/~miklos/DAS).

NMR measurement of spores

For the preparation of cultures, approximately 10^7 spores were inoculated onto 25 ml SFM agar and incubated at 30 °C for 7 days. For each strain, spores from three SFM agar plates were collected in 15 ml H_2O, spores harvested by centrifugation at 3000 rpm for 15 min and supernatant and pellet separated. Spores and spore washout samples were frozen at -80 °C and dehydrated in a freeze dryer for two days. 20 mg of each sample was then re-dissolved in 500 µl D_2O-phosphate buffer and 500 µl CD_3OD, sonicated for 30 minutes for NMR analysis. 0.03% of 3-(trimethylsilyl) propionic acid-d4 sodium salt (TSP) was added to D_2O-phosphate buffer as internal marker. All experiments

were carried out in quintuplicate.

NMR was performed on a 600 MHz Bruker DMX-600 spectrometer (Bruker, Karlsruhe, Germany) operating at a proton NMR frequency of 600.13 MHz. Detailed NMR parameters were used as previously described (Kim *et al.*, 2010). Methanol-*d4* was used as the internal lock. Each ^{1}H NMR spectrum consisted of 128 scans requiring 10 min and 26 sec acquisition time with the following parameters: 0.16 Hz/point, pulse width (PW) = 30° (11.3 μsec), and relaxation delay (RD) = 1.5 sec. A pre-saturation sequence was used to suppress the residual H_2O signal with low power selective irradiation at the H_2O frequency during the recycle delay. FIDs were Fourier transformed with LB = 0.3 Hz. The resulting spectra were manually phased and baseline corrected, and calibrated to MeOH- *d*4 at 3.3 ppm, using XWIN NMR (version 3.5, Bruker).

^{1}H NMR spectra were manually phased, baseline corrected and calibrated. ^{1}H-NMR spectra were further automatically converted to ASCII files using AMIX (v. 3.7, Bruker Biospin). Spectral intensities were scaled to total intensity and the region of δ_H 0.3-10.0 was reduced to integrated regions of width (0.04 ppm). The regions δ_H 4.7 - 5.0 and δ_H 3.30 - 3.34 were excluded from the analysis because of the residual signal of H_2O and methanol-*d4*, respectively. Data were extracted after acquiring the spectra by "binning" or "bucketing", in which spectra are split into discrete regions and integrated (Jellema *et al.*, 2009). Principal component analysis (PCA) was performed with the SIMCA-P software (v. 13.0, Umetrics, Umeå, Sweden) with scaling methods (Kim *et al.*, 2010).

RESULTS

SNP analysis of *S. griseus* SY1 reveals a mutation in a novel cell division-related gene

To identify the mutations in *S. griseus* SY1 relative to its parent *S. griseus* NRRL B2682, both strains were sequenced by Illumina paired end sequencing, and compared to the wild-type strain *S. griseus* IFO13350 (Ohnishi *et al.*, 2008). This revealed around 100 single nucleotide permutations (SNPs) between SY1 and the published sequence of the wild-type strain (not shown). A single SNP stood out, which was a nonsense mutation in gene SGR_6142, the first gene of a likely operon of hypothetical genes encoding membrane proteins; the mutation results in a premature translational stop, whereby Gln7 codon CAG was changed into a TAG stop codon. This will most likely also affect the expression of the downstream genes SGR_6143 and SGR_6144. The orthologs of this gene cluster in *S. coelicolor* are SCO1387-1385. Considering their correlation to the morphology in liquid-grown cultures, the genes SGR_6142-6144 and SCO1387-1385 were renamed *lcmA-C* (for liquid culture morphology) (Fig. 1A).

1A

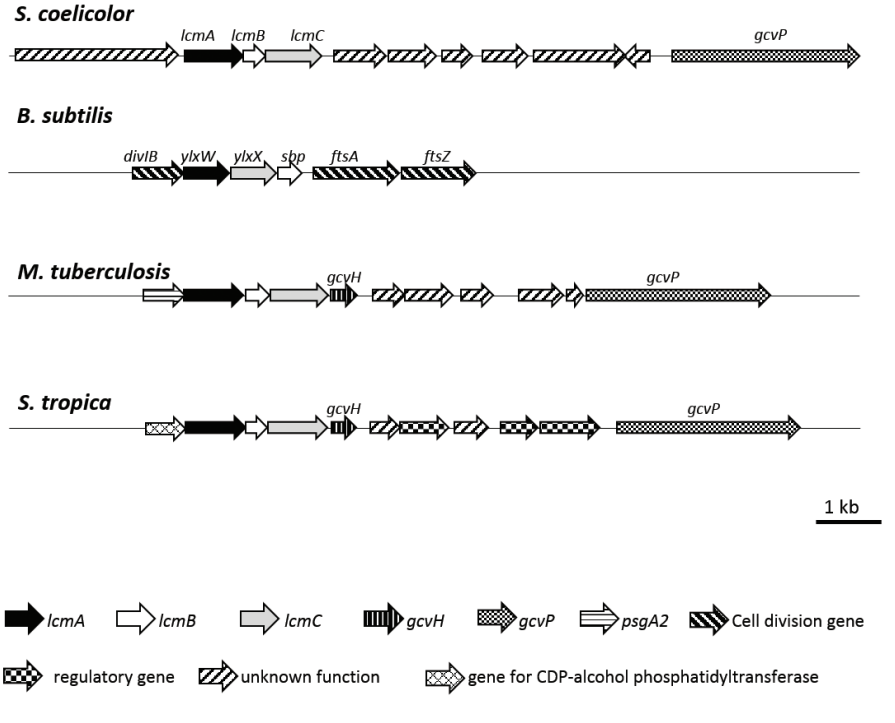

1B

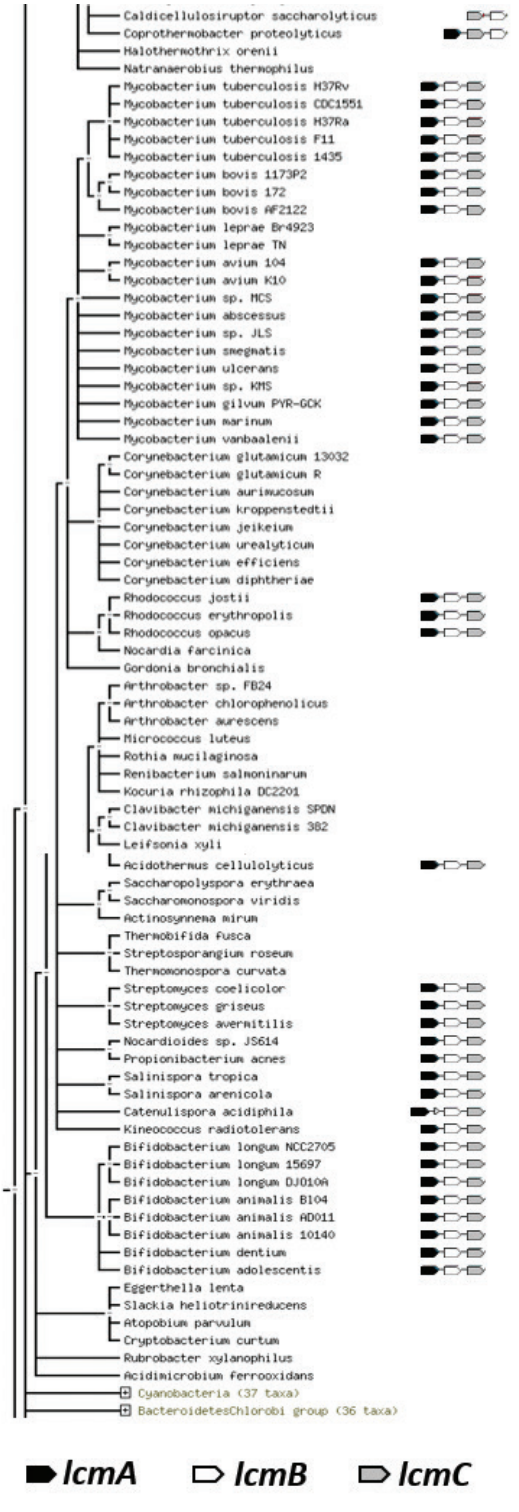

Figure. 1 Gene organization and conservation of *lcm* genes.
(A) Gene organization around the *lcm* genes. The genetic context in *Streptomyces coelicolor* is compared to that in *Bacillus subtilis*, *Mycobacterium tuberculosis* and *Salinispora tropica*. **(B)** Phylogenetic distribution of *lcm* genes in Actinobacteria (output from String engine)

The *lcm* gene cluster

The *lcm* genes are widely conserved among actinobacteria, in a pattern of "all or none", in other words when present they always occur as a cluster (Fig. 1B). With four nucleotides overlap between *lcmA* and *lcmB* and only five nucleotides spacing between *lcmB* and *lcmC*, the three genes most likely form an operon (Romero A *et al.*, 2014). LcmA (301 aa) and LcmC (284 aa) are paralogs based on the significant homology of 30% aa identity and 50% aa similarity between them, in both *S. coelicolor* and *S. griseus*. LcmA and LcmC have a predicted N-terminal transmembrane domain of unknown function (DUF881). Interestingly, LcmC also contains an additional FliH domain, belonging to flagellar assembly proteins. LcmB (110 aa) is a basic protein with four predicted transmembrane domains.

The orthologs of *lcmA*, *lcmB* and *lcmC* in *B. subtilis* are *ylxX*, *sbp* and *ylxW*, respectively, which are located downstream of *divIB* in the *dcw* cluster with genes involved in cell division and cell-wall synthesis (Rowland *et al.*, 1995; Cha and Stewart, 1997) (Fig. 1A). Temperature-sensitive mutant *B. subtilis tms-12* has a sporulation defect at elevated temperatures (Breakefield and Landman, 1973; Miyakawa and Komano, 1981). The *tms-12* mutation in *B. subtilis* mutates *divIB*, and surprisingly, like the mutation in *lcmA*, was also a nonsense mutation close to the start of the gene, resulting in elimination of 93 residues of the DivIB protein (Beall and Lutkenhaus, 1989). *divIB* lies immediately upstream of *ylxX*, and considering the translational coupling between *divIB* and *ylmX*, with overlapping stop and start codons (ATGA arrangement, whereby ATG is the start codon for *ylmX* and TGA the stop codon for *divIB*), the nonsense mutation in *divIB* most likely affects the expression of the downstream genes *ylxX*, *ylxW* and *sbp*. These data suggest that the *Streptomyces lcm* locus may play a role in cell division, apparently correlating with the observed fragmenting phenotype of spontaneous mutant SY1 of *S. griseus*.

Deletion of the *lcm* genes accelerates development in *S. coelicolor*

To investigate the effect of the mutation in *lcmA* on growth and development of wild-type *S. griseus* IFO13350 and of *S. coelicolor* M145, mutants of the *lcmABC* operon were created, so as to obtain single mutants and a cluster deletion. The strategy and plasmids used for gene replacements and mutations are described in detail in the Materials and Methods section. To introduce the corresponding nonsense mutation found in SY1 in *S. coelicolor lcmA*, the CCA codon for amino acid residue Pro7 was changed to a TGA stop codon, resulting in strain GAL59. Deletion mutants GAL56 (*S. coelicolor* M145 Δ*lcmA*),

GAL57 (*S. coelicolor* M145 Δ*lcmB*) and GAL58 (*S. coelicolor* M145 Δ*lcmC*) were also obtained, as well as cluster deletion mutant GAL60. Similarly, the CAG codon for amino acid residue Gln7 of *S. griseus lcmA* was changed to a TAG stop codon, resulting in strain GAL59-sg. Mutants GAL56-sg (*S. griseus* IFO13350 Δ*lcmA*) and GAL60-sg (*S. griseus* IFO13350 Δ*lcmABC*) were created using *S. griseus* IFO13350 as the parental strain.

The morphology all mutants and their parental strains were studied in submerged culture. Despite the strong phenotype of *S. griseus* SY1, none of the mutants of *S. coelicolor* or *S. griseus* showed mycelial fragmentation under the conditions tested (Fig. 2A). Dense clumps were produced by all mutants, similar as the parents *S. griseus* IFO13350 or *S. coelicolor* M145. Light microscopy did not identify major changes in development in any of the *lcm* mutants in *S. coelicolor* or *S. griseus*, producing abundant grey-pigmented spores, very similar to the parental strains, although some mutants consistently sporulated earlier than the parent. Further studies on the effect of the *lcm* mutations were done only in *S. coelicolor*.

2A

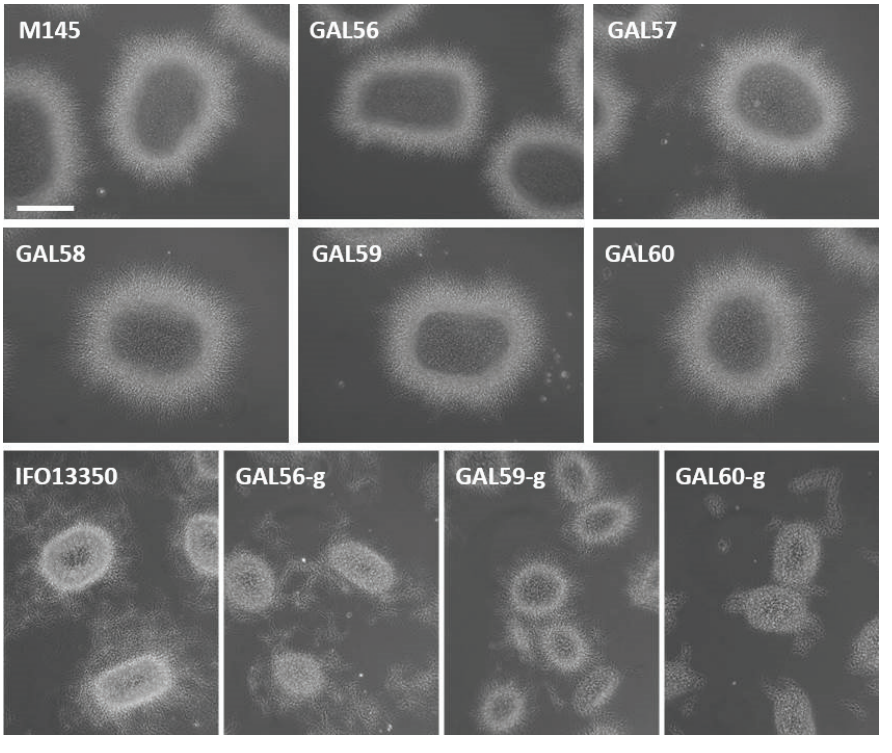

2B

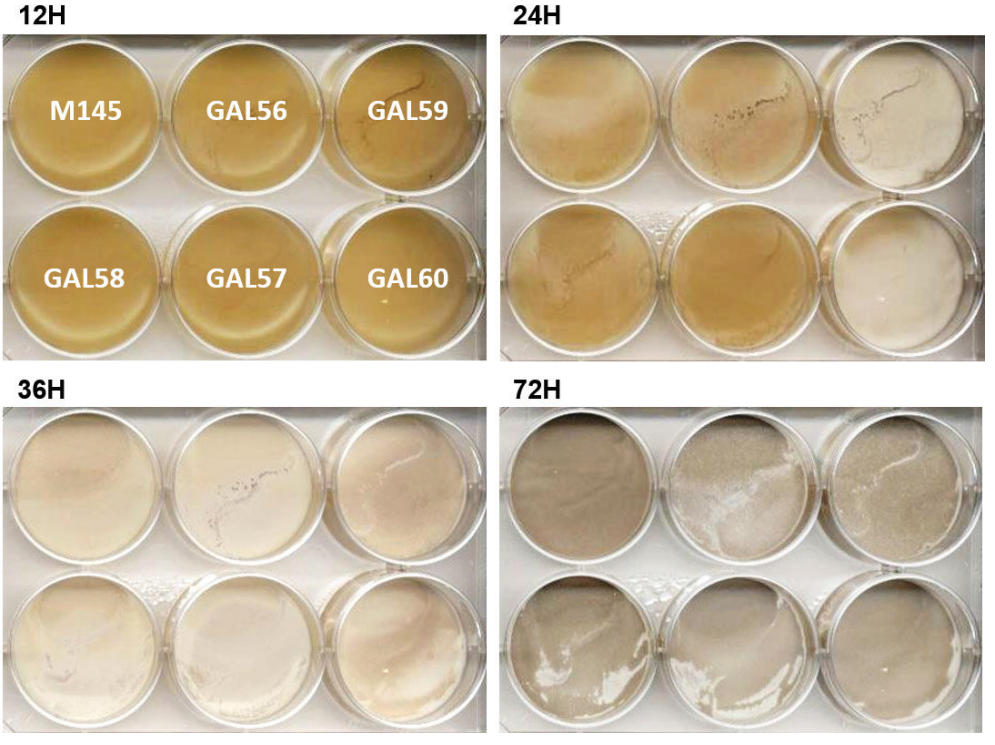

Figure. 2 Morphology of *S. coelicolor* and *S. griseus* and their *lcm* mutants.
(A) phase-contrast micrographs of liquid-grown cultures of wild-type *S. coelicolor* M45, and its mutant derivatives GAL56 (Δ*lcmA*), GAL57 (Δ*lcmB*), GAL58 (Δ*lcmC*), GAL59 (*lcmA**, nonsense mutation) and GAL60 (Δ*lcmABC*), and wild-type *S. griseus* IFO13350 and its mutants GAL56-g (Δ*lcmA-sg*), GAL59-g (*lcmA*-sg* and GA60-g (Δ*lcmABC-sg*). Bar, 50 μm. **(B)** Growth of *S. coelicolor* M145 and its *lcm* mutants of M145 on SFM medium at different time points.

To investigate whether timing of development was indeed affected in these mutants, spores of *S. coelicolor* mutants were counted using a haemocytometer, and the titer in terms of colony forming units (cfu/ml) determined. The same amount of viable spores was then taken for each strain and plated onto SFM agar plates at 30^0C. The plates were photographed in the incubator at 30 min intervals. Interestingly, strains GAL59 (M145 *lcmA**) and GAL60 (M145 Δ*lcmABC*) produced abundant white-pigmented aerial hyphae after only 24 h of growth, which is much earlier than the wild-type strain (Fig. 2B). After 36 h, GAL59 and GAL60 already entered sporulation, as indicated by the grey pigmentation, while the parent and the other mutants had now initiated aerial growth. After 72 h all strains had completed development (Fig. 2B). On R5 agar media, all mutants produced comparable amount of the pigmented

antibiotics undecylprodigiosin (red) and actinorhodin (blue) as the wild-type strain, but again strains GAL59 and GAL60 developed much earlier than the other strains, consistent with the results obtained for growth on SFM agar (data not shown). Taken together, the *lcmA** and *lcmABC* mutants had accelerated development by at least half a day. However, since none of the single deletion mutants was affected, the accelerated sporulation was most likely due to the absence or altered expression of at least two of the genes.

The *lcm* locus is involved in sporulation

Cryo-scanning electron microscopy (SEM) was used to examine the spores in detail. Wild type *S. coelicolor* M145 produced typical chains of uniform spores. All *lcm* mutants also sporulated abundantly, in line with the light microscopy. However, variations in spore sizes were seen in all mutants (Fig. 3). To quantify this, the average spore length was calculated based on a hundred spores per strain (Table 4). The average length of wild-type spores was 0.97 ± 0.13 μm, while spores of single *lcm* gene deletion mutants GAL56, GAL57 and GAL59 were around 80-110 nm longer. However, the *lcmA** and the *lcmABC* cluster deletion mutants produced significantly larger spores, namely on average 1.12 ± 0.20 μm.

In an attempt to complement the mutants, construct pGWS778, which is a low-copy number vector harboring the entire *lcmABC* cluster and its native promoter region, was introduced into GAL59 and GAL60, generating strains GAL68 (GAL59 + pGWS778) and GAL69 (GAL60 + pGWS778). In line with the notion that the sporulation defect was due only to mutations in the *lcm* cluster, the average spore length of the transformants was reduced to values close to those of the wild-type strain M145, namely to 0.99 ± 0.15 μm and 1.03 ± 0.14 μm, respectively. This established that the genes in the *lcm* locus are involved in sporulation.

Table 4. Spore length of *S. coelicolor* M145, its *lcm* mutants and complemented strains.

	M145	GAL56	GAL57	GAL58	GAL59	GAL60	GAL68	GAL69
Spore length (μm)	0,97 ± 0.13	1.05 ± 0,15	1.08 ± 0.17	1.08 ± 0.23	1.12 ± 0,20	1.12 ± 0.20	0.99 ± 0,15	1.03 ± 0,14

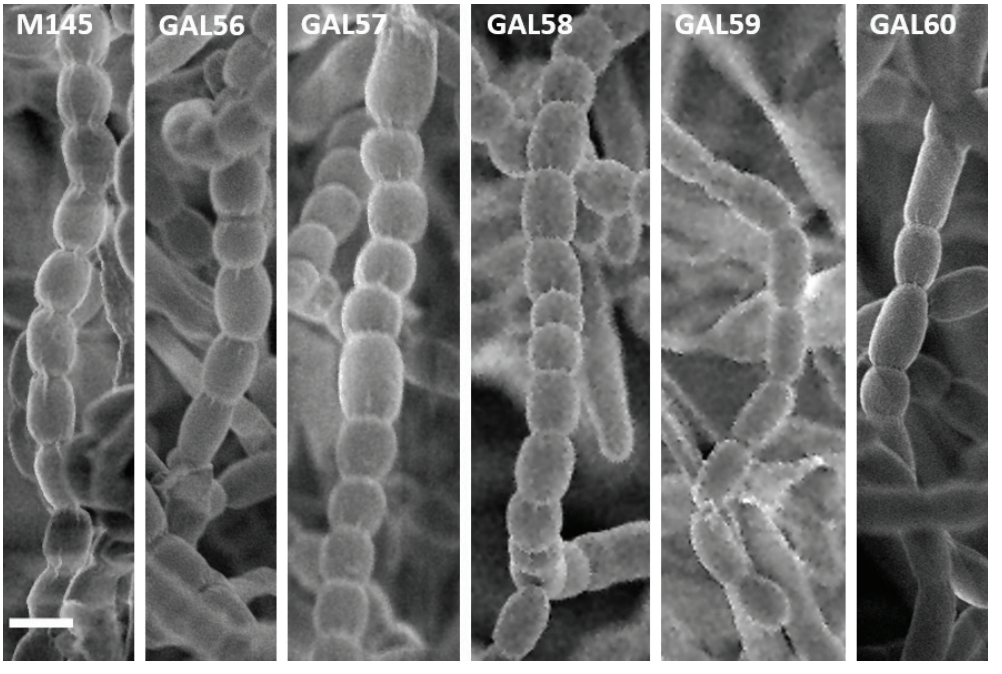

Figure 3. Scanning electron micrographs of spores of wild type *S. coelicolor* M145 and its *lcm* mutants. For strains see legend to Fig. 2A. Cultures were grown on SFM agar plates for 5 days at 30^0C. Bar, 1 μm.

lcm mutants produce heat-sensitive spores

Considering the changes to sporulation seen in the mutants, we examined the stress resistance of the spores. To test heat resistance, around 400 cfu were incubated at 60°C for 10 minutes and plated onto SFM agar plates. Approximately 47% of the wild-type spores survived the heat treatment (Fig. 4A). The survival rates for spores of single deletion mutants GAL56 (Δ*lcmA*), GAL57(Δ*lcmB*) and GAL58 (Δ*lcmC*) were 43%, 40% and 42%, which indicates slightly lower heat resistance as compared to spores of the parent. The *lcmA** and *lcmABC* mutants were less resistant to the heat treatment, with 35% and 36% of spores surviving the heat treatment, respectively. Spores of GAL68 and GAL69, which are GAL59 and GAL60 complemented with pGWS778, showed very similar heat survival rate as wild-type spores (Fig. 4A). This suggests that the increased sensitivity to heat treatment was most likely due to changes in the *lcm* locus.

Transmission electron microscopy (TEM) was applied to study the spores in more detail. Again, the TEM confirmed the large variation in spore sizes in

some of the *lcm* mutants (Fig. 4B). Furthermore, a white crystalline material was often seen to accumulate near the wall of mutant spores (Fig. 4B, arrows). This may be explained as accumulation of the fixative inside the mutant spores (with weaker and hence more easily penetrated spore walls) used for sample fixation prior to TEM imaging. Additionally, while the spores of M145 and of single mutants GAL56, GAL57 and GAL58 had a typical thick cell wall, strain GAL59 that carries non-sense mutation *lcmA** and the *lcm* cluster mutant GAL60 had a thinner cell wall (Fig. 4B). Such a thinner cell wall could explain the increased heat sensitivity, the penetration of fixative and the accelerated germination. The latter corresponds to previous observations that germination efficiency correlates to cell-wall thickness (Piette *et al.*, 2005).

4A

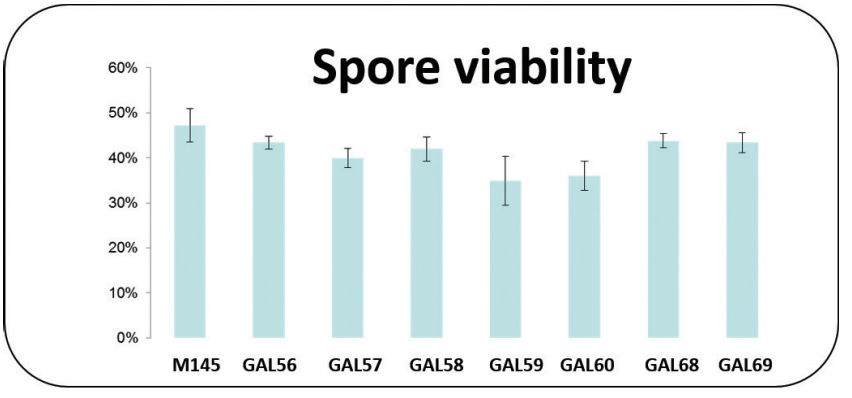

4B

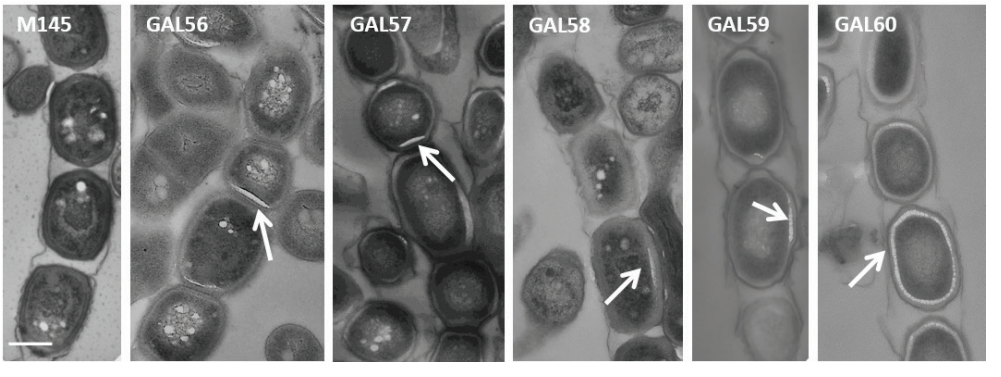

Figure 4. Spore viability after heat shock (A) and transmission electron micrographs (B) of spores of *S. coelicolor* M145 and its *lcm* mutants. For transmission electron microscopy, strains were grown on SFM agar plates for 5 days at 30^{0}C. White crystalline material in *lcm* mutants are indicated by arrows. For strains see legend to Fig. 2A. Bar, 500 nm.

lcm genes and cell-wall assembly

To further study the *lcm* mutants *in vivo*, fluorescence microscopy was applied on 72 hr old SFM-grown strains GAL56, GAL57, GAL58, GAL59, GAL60 and M145 to analyze cell wall, membrane and nucleoid distribution. Peptidoglycan precursors were stained with FITC-WGA, membranes with FM5-95, and DNA with DAPI. Mutants GAL56, GAL57 and GAL58 showed a very similar pattern of cell wall and membrane distribution as the wild type strain, although some variation in spore sizes was observed (Fig. 5A). Conversely, mutants GAL59 (Fig. 5B) and GAL60 (Fig. 5B) produced much larger spores, consistent with the SEM and TEM analysis. Interestingly, the large spores sometimes contained mis-localized cell-wall material, perhaps as a result of incomplete septation; this suggests that the *lcm* gene cluster may play a role in spore maturation and completion of septation. Indeed, we regularly observed incomplete septa in both the *lcmA** mutant and the *lcmABC* deletion mutant (arrows in Fig. 5B).

5A

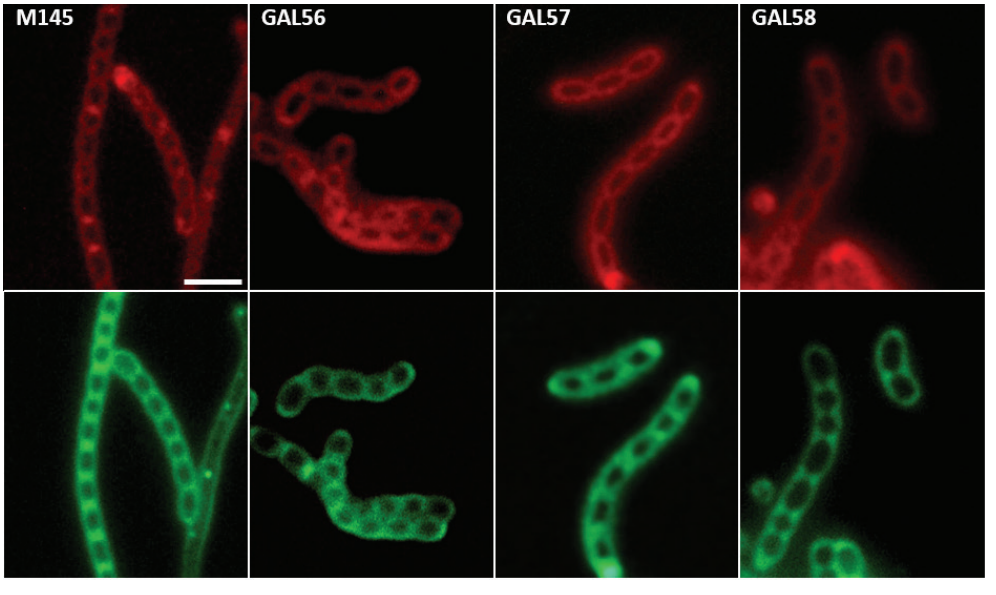

5B

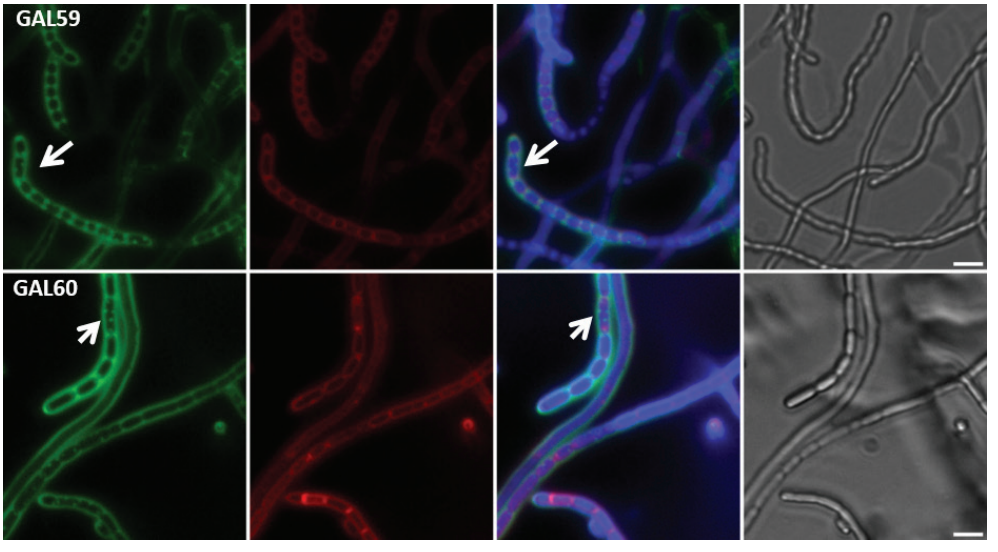

Figure 5. Fluorescence micrographs of *S. coelicolor* M145, and its *lcm* mutants. The samples were stained for cell wall (FITC-WGA, green), membrane (FM5-95, red), or DNA (DAPI, blue; co-stained with FITC-WGA and FM5-95) and corresponding light images. Incomplete septation in GAL59 and GAL60 is indicated by arrows. For strains see legend to Fig. 2A. Bar is 3 μm.

Localization of the Lcm proteins

To examine the localization of the Lcm proteins in the hyphae of *S. coelicolor*, integrative plasmids were constructed, harboring *lcmA, lcmB* or *lcmC* under the control of the *ftsZ* promoter, and fused immediately upstream of *egfp* so as to create translational fusions (see Materials and Methods section). Constructs pGWS768, pGWS769 and pGWS770, which express LcmA-eGFP, LcmB-eGFP and LcmC-eGFP, respectively, were then introduced into *S. coelicolor* M145.

We failed to detect specific localization of LcmA, LcmB or LcmC foci in vegetative hyphae (not shown). However, in aerial hyphae LcmA-eGFP either formed distinct foci, including one at the tip (Fig. 6A), or was more dispersed (Fig. 6A). This indicates that LcmA localizes in a stage-specific manner, and perhaps that the 'random' localization precedes the focal localization, but to determine the precise order requires live imaging. A similar localization pattern as seen for LcmA-eGFP was also observed for LcmB-eGFP and LcmC-eGFP at the stage prior to sporulation (Fig. 6A). Once sporulation had started, and septa ladders became visible, LcmA-eGFP, LcmB-eGFP and LcmC-eGFP localized in a ladder-like pattern close to the septa (Fig. 6B). Interestingly, the

paralogous proteins LcmA and LcmC localized in foci at either side of the center of the septum and in an oblique arrangement, with an imaginary line through the foci forming an approximately 45° angle with the septum (Fig. 6B). However, LcmB-eGFP overlapped the septum (Fig. 6B). The localization of the Lcm proteins could be classified in three groups: overlap with septum staining, no overlap with septum staining and cross-septum staining (*i.e.* foci at either side of the septum). LcmA-eGFP (92%) and LcmC-eGFP (79%) primarily formed foci across the septum, while LcmB-eGFP (89%) dominantly overlapped septum staining (Table 5). This suggests that perhaps the membrane protein LcmB assembles at the septum site, and interacts with LcmA and LcmC at the centre of the septum. No localization of LcmA, LcmB and LcmC was detected in mature spores.

6A

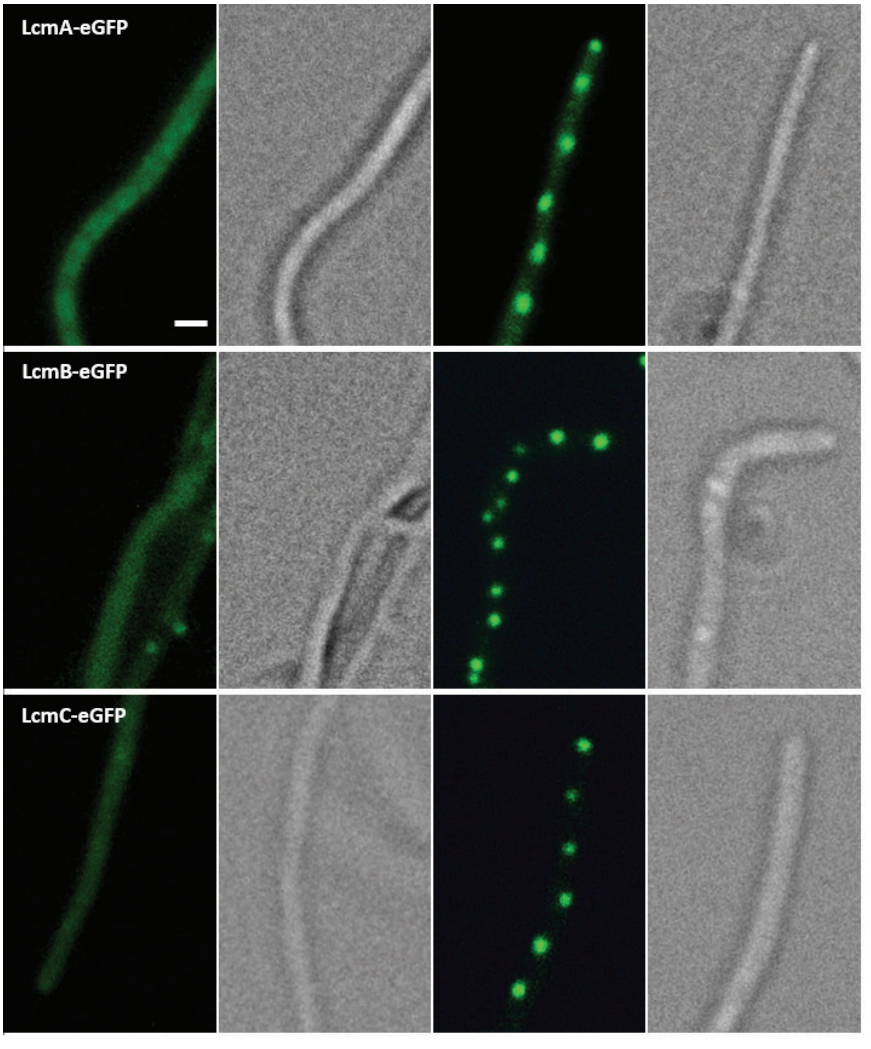

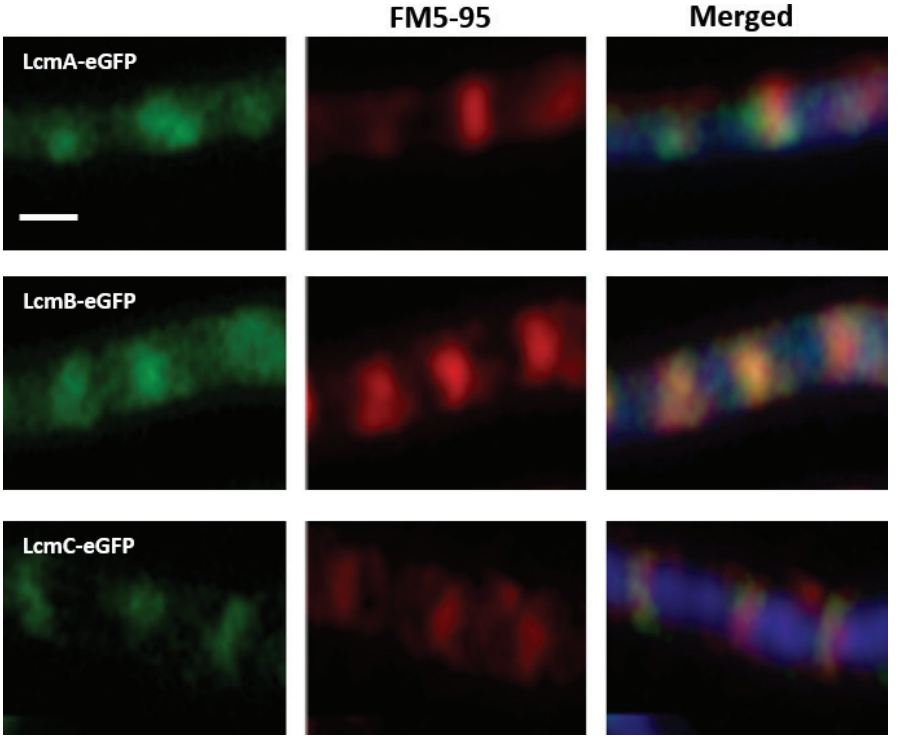

Figure 6. Localization of LcmA-eGFP, LcmB-eGFP and LcmC-eGFP at the septa. Aerial hyphae of *S. coelicolor* M145 were imaged by fluorescence microscopy visualizing eGFP fusion proteins of LcmA, LcmB and LcmC. **(A)** FM of the eGFP fusion protein in young aerial hyphae (diffuse localization; left) and in pre-mature spores (right). For each image both FM and light micrographs are presented. Bar, 1 μm. **(B)** Close-ups of eGFP fusions (left) and membrane staining (FM5-95; middle), together with the merged images (right), showing localization of Lcm proteins at the septa.

Table 5. Statistical analysis of the localization of Lcm proteins relative to the sporulation septa.

Position of foci	LcmA-eGFP	LcmB-eGFP	LcmC-eGFP
Overlap with septum	**2%**	**89%**	**5%**
Not at the septa	7%	4%	17%
Cross septum	**92%**	8%	**79%**

Phylogenetic linkage to *gcv* genes

In actinomycetes the *lcm* cluster is typically associated with genes of the glycine cleavage system, and in particular *gcvP* or *gcvH* (Fig. 1A). In several actinomycetes, including *Salinispora*, *Kineococcus* and *Catenulispora*, *gcvH* lies immediately downstream of *lcmC*, while *gcvP* (SCO1378) lies 7 genes downstream of *lcmC* in *S. coelicolor*. This suggests possible functional linkage be-

tween the *lcm* and *gcv* genes. The glycine cleavage system (GCS) is expressed in response to high concentration of the amino acid glycine, to recycle glycine (Kikuchi *et al.*, 2008). This is important as glycine is toxic for many microorganisms at higher concentrations (Hishinuma *et al.*, 1969). Considering that glycine is an important part of the cell wall, forming glycine bridges between the peptidoglycan strands, and also affects pellet morphology of streptomycetes, we analyzed if the *lcm* genes played a role in glycine-related metabolism. Therefore, a null mutant of *S. coelicolor gcvP* (called GAL61) was obtained by replacing the gene with the apramycin resistance cassette *aac(3)IV* (see Materials and Methods section). Expectedly, this mutant was inhibited by higher glycine concentrations, as described previously for *gcv* mutants ΔUTR-T and ΔUTR-P of *S. griseus* IFO13350 (Tezuka and Ohnishi, 2014) (Fig. 7). However, none of the *lcm* mutants of *S. coelicolor* or *S. griseus* showed significant changes in terms of glycine sensitivity as compared to the parental strains (Fig. 7), suggesting that the *lcm* genes are not required for glycine catabolism.

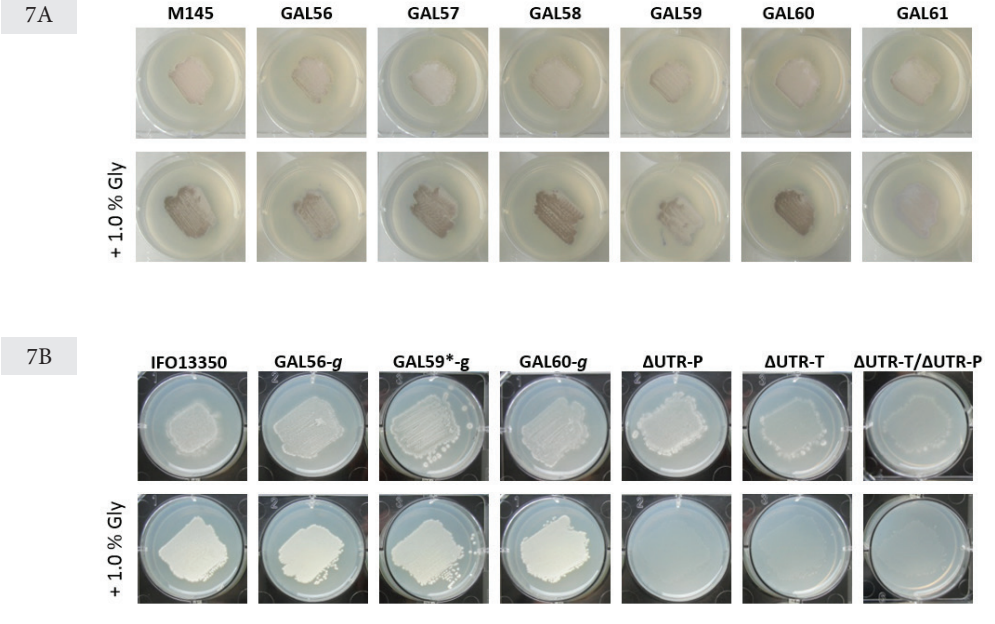

Figure 7. Effect of glycine on growth. (A) *S. coelicolor* M145 and its *lcm* and *gcvP*-null mutants on MM agar (with only agar as carbon source) or on MM agar containing additional 1% (w/v) glycine. **(B)** Growth of *S. griseus* IFO13350, its *lcm* mutants and a glycine riboswitch-null mutants on SMM agar (with only agar as carbon source) or on SMM agar containing additional 1% (w/v) glycine. Photos were taken after 4 days incubation at 30°C.

PCA analysis of metabolic profiles by proton NMR

NMR was applied to metabolically investigate spores of the *lcm* mutants. Strains GAL59 (*lcmA**) and GAL60 (Δ*lcmABC*) were selected since these two strains exhibited the most obvious changes as compared to the wild-type strain. Strain GAL61 (M145 Δ*gcvP* (::*aac(3)IV*)) was also included in NMR experiment as a control. To get full metabolic profiles for each strain, the spore pellet and supernatant were prepared as described in the Materials and Methods, followed by NMR spectroscopy. Five replicates were used for each experiment, so as to guarantee good statistical value of the data. Metabolite variations of samples from different strains were identified by principal component analysis (PCA). PCA is an unbiased and unsupervised method which is able to reduce the dimensionality of datasets. All NMR signals of the data sets were simplified to Principal Component 1 (PC1) and Principal Component 2 (PC2). Via this method, most NMR information was covered and spread out into a two-dimensional diagram (Kim *et al.*, 2010; Jellema *et al.*, 2009).

In the PCA score plot of spores, mutant strains and wild type were mainly separated by PC1 (Fig. 8A). Metabolites from the parental strain *S. coelicolor* M145 were predominantly found in the neutral part of the plot, *gcv* mutant GAL61 was at the negative side of PC1, while *lcm* mutants GAL59 and GAL60 were mostly at the positive side of PC1. The column loading plot of PC1 clearly showed large accumulation of glycine in GAL61 spores, in line with the mutation of the glycine cleavage system (Fig. 8A). The level of trehalose was also sharply increased in GAL61 spores. The accumulation of trehalose in *Streptomyces* spores enhanced the resistance to heat and postponed time of germination (McBride and Ensign, 1987). GAL59 and GAL60 showed a wide range of changes in the metabolic profiles, with 2-phosphoglycerate as a striking example. 2-phosphoglyceric acid is the intermediate product in the conversion of glucose to pyruvate, and the observed accumulation of 2-phosphoglycerate suggests a major change in glucose metabolism in the mutants.

In the PCA score plot of the supernatants, again mutants and wild-type were well separated, this time by PC2. Wild-type and GAL61 were at the positive side of PC2, while wild-type supernatants were close to the neural region; supernatants of GAL59 and GAL60 were both at the negative side of PC2 (Fig. 8B). A large amount of glycine was found in the supernatant of *gcv* mutant GAL61, and also of lactic acid (Fig. 8B). Consistent with the column loading plot for the spores, GAL59 and GAL60 once more showed significant changes in the metabolite profiles than *gcv* mutant GAL61. Among others, higher concentrations of the sugars mannitol and raffinose were found in the supernatant of GAL59 and GAL60 as compared to supernatants of the wild-

type strain, while the level of 2-phosphoglycerate was also higher in the supernatant of GAL59 and GAL60. This was in line with the changes seen in the spore fractions. The distinct spore and supernatant profiles observed in the PCA score plot strongly suggests that mutation or deletion of the entire *lcm* cluster causes major metabolic changes. The PCA loading plots showed that in particular the profiles of sugars and amino acids (but not glycine) were altered in GAL59 and GAL60.

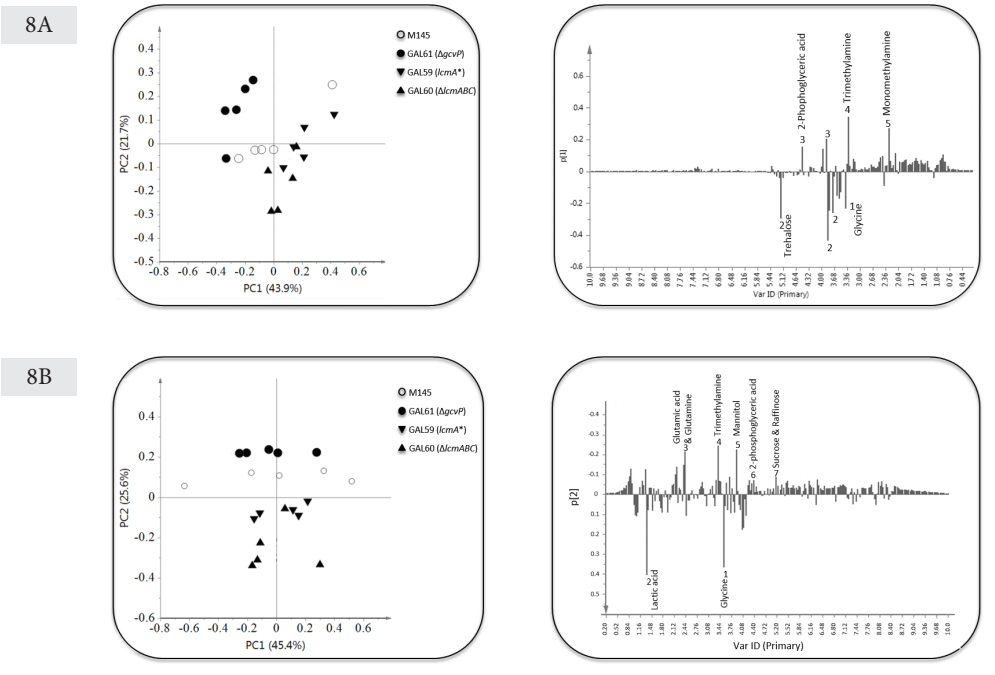

Figure 8. Metabolome analysis of spore metabolites by PCA. PCA analysis and corresponding loading plots are shown for **(A)** spores and **(B)** supernatants from spore preps. Extracts and supernatants from spores of wild type *S. coelicolor* M145, GAL59 (*lcmA**), GAL60 (Δ*lcmABC*) and GAL61 (Δ*gcvP*) were analyzed.

DISCUSSION

Streptomycetes are mycelial microorganisms that reproduce via sporulation on solid media. In addition, a significant number of the streptomycetes can also sporulate in submerged culture (Girard *et al.*, 2013). The factors that determine mycelial morphogenesis in submerged cultures are still largely unknown, although altering the expression of the cell division activator SsgA or deletion of cell matrix genes like *cslA* for cellulose synthase-like protein CslA or *chp* for the chaplin spore-coat proteins results in fragmentation of the mycelia and in some cases even submerged sporulation (van Dissel *et al.*, 2014). Important clues could come from the analysis of spontaneous mutants with altered morphology. One such mutant is *S. griseus* strain SY1, which was derived from wild-type *S. griseus* by random mutagenesis (Kawamoto and Ensign, 1995), and fragments and sporulates in rich liquid media, while wild-type *S. griseus* only produces spores after nutritional shift-down. SNP analysis showed that *S. griseus* SY1 contains among others a non-sense mutation in the gene *lcmA,* which is the first gene of an operon of three genes (*lcmABC*). This change probably has a detrimental effect on the expression of all three genes in the cluster, as the genes likely form an operon, with *lcmA* and *lcmB* translationally coupled. To establish the role of the *lcmABC* gene cluster in the medium-dependent submerged sporulation of *S. griseus*, a series of mutants was created in both *S. griseus* and in our model system *S. coelicolor*. These mutants were gene deletion mutants for either *lcmA*, *lcmB* or *lcmC*, or a complete cluster deletion mutant, as well as a mutant (designated *lcmA**) with the same non-sense mutation found in SY1 (replacing codon 7 by a stop codon). While the *lcmA** strain containing the nonsense mutation and the *lcmABC* deletion strain showed altered sporulation on solid cultures, with larger spores, thinner spore walls and accelerated development, none of the mutants had significantly altered morphology in submerged cultures, regardless of whether the *lcm* mutants were created in *S. coelicolor* or in *S. griseus*. This suggests that at least one other mutation sustained after random chemical mutagenesis was responsible for the hypersporulating phenotype of *S. griseus* SY1. Considering that some 100 SNPs were found in SY1 relative to the parental strain *S. griseus* NRRL B2682 (a derivative of the wild-type strain), and the fact that the phenotype may have been the result of multiple mutations, the search for the responsible gene(s) was abandoned. However, based on the strong connection between the *lcm* genes and sporulation, we expect that the *lcmA** mutation will at least have contributed to the hyper-sporulating phenotype of *S. griseus* SY1.

What then is the role of *lcmABC* in sporulation? All three genes encode predicted membrane proteins, and suggestively, in *Bacillus* the genes lie downstream of the cell division gene *divIB* in the *dcw* cluster of genes for division and cell-wall synthesis. Interestingly, localization studies on eGFP fusion protein showed that all three proteins localize close to or at the septum, whereby LcmB-eGFP overlaps the sporulation septa, while LcmA-eGFP and LcmC-eGFP produce foci on either side of the center of the septa. This localization suggests that perhaps LcmABC play a role in septum closure, although more data are required to establish their precise roles in cell division. Also, the sequence of their localization pattern in younger aerial hyphae requires more extensive imaging, and in particular live imaging, as it is very difficult to judge the exact stage of development of aerial hyphae where indentation (*i.e.* sporulation) has not yet started.

The observed accelerated growth for the *lcm*A* and *lcmABC* mutants on solid media may among others be explained by the altered (and somewhat thinner) spore wall of the mutants, since this would facilitate more rapid germination (Piette *et al.*, 2005). Phylogenetic evidence shows strong correlation between the *lcm* genes with the *gcv* genes that encode components of the glycine cleavage system, although in contrast to *gcv* mutants, *lcm* mutants did not show enhanced sensitivity to glycine. However, analysis of the spores and spore supernatants of the lcmA* and *lcmABC* mutants by NMR-based metabolomics did reveal major changes in metabolic composition, as shown by the PCA analysis of five independent replicates. In particular, the mutants showed altered in sugar and amino acid metabolism. Further analysis of the Lcm proteins, such as identification of possible interaction partners as well as elucidation of the molecular basis for the metabolic changes observed in the mutants, should shed further light on their role during sporulation of streptomycetes.